

PHOTOGRAMMETRIC RECONSTRUCTION OF ADOBE ARCHITECTURE AT TÚCUME, PERU

M. Sauerbier^a, M. Kunz^b, M. Fluehler^b, F. Remondino^a

^a Swiss Federal Institute of Technology
Institute of Geodesy and Photogrammetry,
CH-8093 ETH Hoenggerberg
www.photogrammetry.ethz.ch
(martin.sauerbier, fabio.remondino)@geod.baug.ethz.ch
^b(mela, fluehlma@student.ethz.ch)

Commission V, Working Group V/6

KEY WORDS: Aerotriangulation, DEM, Bundle Adjustment, Cultural Heritage, Orthoimage, Visualization

ABSTRACT:

In northern Peru, near the city of Chiclayo, a unique complex of adobe architecture exists, built since about 3000 years ago until it was finished during the Sicán period in the 13th century A.D. The archaeological investigations of the adobe buildings have not been completed until now, therefore, there is an interest concerning a photorealistic 3D model of the complex in the archaeological community involved into scientific research at Túcume. As the adobe buildings are heavily affected by wind erosion, the architecture should be modelled as good as possible in an unaffected state. For this reason, aerial imagery from the years 1949 and 1983 were acquired from the Peruvian SAN (Servicio Aerofotográfico Nacional, Lima), which show the adobe complex in two different states. As no control points existed for the 1949 images, two maps and the 1983 imagery had to be used for their orientation. The orientation of the 1983 images was accomplished on an analytical plotter WILD S9, while for the orientation of the 1949 images both, the analytical plotter and a digital photogrammetric workstation Virtuozo 3.1, were used. The photogrammetric products derived from the oriented 1949 images are a manually measured DTM, an automatically generated DSM, an orthomosaic and a photorealistic 3D model produced using two different visualization software packages, Skyline Terra Builder / Explorer Pro and ERDAS Imagine Virtual GIS. The 3D model now can serve archaeologists and other scientists as a means for documentation, analysis and presentation of the cultural heritage site of Túcume in a state of preservation as in 1949.

1. INTRODUCTION

1.1 Area of investigation

In the region of Túcume in northern Peru (Figure 1), nearby the cities of Chiclayo and Trujillo, the so-called “Pyramids of Túcume” represent a unique example of adobe architecture built during different periods of pre-hispanic cultures. About 3000 years ago, people started to construct various buildings until they were completed during the 13th century A.D. in the period of Sicán, and later also used by the Incas. From the Cerro La Raya, a characteristic hill in the centre of the site, 26 adobe buildings are visible, the largest one, *Huaca Larga*, with a length of 545m, 110m of width and 21m of height. On top of *Huaca Larga*, the Incas constructed a stone building. During excavations in the last years, tombs, reliefs and coloured wall drawings were found. Besides the pyramids, the complex contains platforms, citadels, residential areas and cemeteries. The fact that Túcume has been an urban settlement area for the cultures of Lambayeque, Chimú, Sicán and Inca consecutively makes it one of the most important cultural heritage sites of the ancient Peru.



Figure 1: Túcume, northern Peru (Fluehler, 2004)

Due to the impact of wind, especially the side walls of the pyramids are heavily eroded, a process that slowly destroys the adobe buildings. Therefore, a complete documentation of the site in a more or less original state of preservation is a need, not

only for archaeological research but also for presentation purposes, e.g. in museums. Nowadays, the region of Túcume is an agricultural, rural area with settlements in the direct neighbourhood of the adobe complex.

1.2 Available Data

The first step in the photogrammetric reconstruction workflow is the acquisition of image data and additional data to process the images, with the aim of a generation of a photorealistic 3D model. Aerial images could be acquired from the Peruvian SAN. For our purposes, two series of aerial B/W images, taken during photoflights in the years 1983 and 1949, were chosen. For the 1949 images (no. 977-980), no camera information was available, neither the type of camera nor calibration data. The 1983 images (no. 598, 599, 600) were delivered with a calibration protocol. Both series of aerial images were taken from a flying height of about 1.500m in one strip at an overlap of 60% in flight direction. With a camera constant of about 0.15m and the resulting approximate image scale of 1:10.000 the modelling of details in these images is limited.

Due to the lack of existing control points of high accuracy, topographic maps of the area had to be used to extract points for the absolute orientation of the images of 1983. Two different maps could be acquired from INGEMMET (Instituto Geológico Minero y Metalúrgico, Lima) at scales of 1:5.000 and 1:10.000 from around 1980 (exact date unknown). The 1:5.000 map, which was in fact a copy of unknown scale, could be used for the extraction of height control points as it contained contour lines, but was not suited for the extraction of full control points

due to the unknown scale of the copy. The 1:10.000 scaled map was a composition of a topographic map of the surroundings of the adobe complex and an archaeological map of the adobe complex and *Cerro La Raya*. No information was available of how exactly both maps were integrated and georeferenced. Both, the 1:5.000 and the 1:10.000 scale maps, were generalised strongly especially in the settlement areas which made the extraction of accurate control points difficult. Usually, points can be extracted from a map at 0.2 mm accuracy, which in our case would lead to an estimated object space accuracy for control points extracted from the maps at 1m and 2m, respectively. In our case, these values are too optimistic due to the unknown degree of generalisation of both maps, which nevertheless are the only available information source for orientation data at a suitable scale and therefore had to be used.

1.3 Photogrammetric Workflow

As no control points for the 1949 images could be identified directly in the topographic maps, first the 1983 images had to be oriented using the extracted control points. Later on, corresponding points between the 1949 and the 1983 images should be used for their orientation. Afterwards, DTM and DSM should be derived on an analytical plotter WILD S9 and a digital photogrammetric workstation Virtuozo 3.1 (Supresoft Inc.), respectively, as a basis for orthophoto production and 3D visualisation (Figure 2). Finally, a comparison between the manually measured DTM and the DSM should have been done.

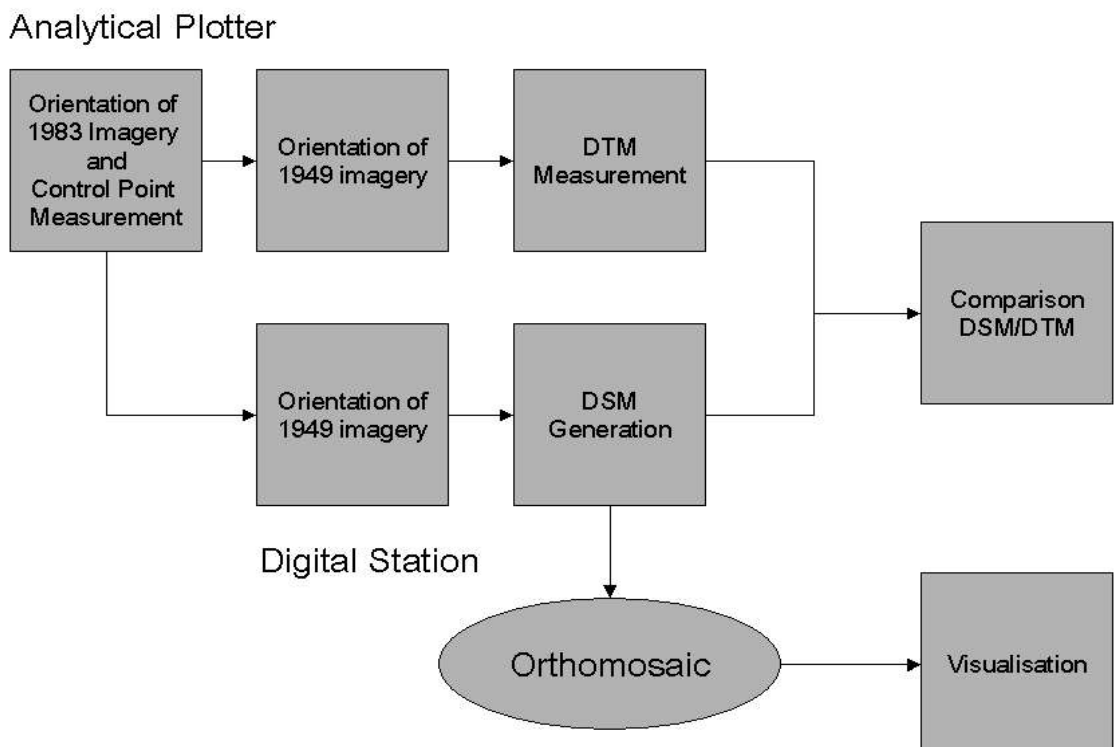


Figure 2: Photogrammetric workflow for 3D model generation

2. IMAGE ORIENTATION

2.1 Control Point Extraction from topographic maps

As mentioned above, control points had to be extracted from two different topographic maps, a process which turned out to be one of the problematic steps in this project. The projection of the maps was UTM Zone 17S with the Provisional South American Datum of 1956. A number of different factors influenced the accuracy of control point extraction from the maps:

- The generalisation, especially of buildings, made it difficult to find common points even between the maps and the 1983 images
- The high change rate of buildings as well as of agricultural areas had the same effect
- The landscape characteristics which shows only few striking features suited for control point extraction
- Confusion of objects
- Visibility of points in the aerial images
- Maps do not display the current state

After various trials using different combinations of extracted control points, 6 points only were suited for an accurate orientation of the images of 1983 (Figure 3). From these 6 points, only the points 1002 and 1009 (Table 1) were full control points, the other 4 could only be used as height control points.

ID	X [m]	Y [m]	Z [m]
1002	626190.00	9280440.00	42.20
1009	628850.00	9280245.00	49.20
2001	627256.16	9280372.63	44.50
2002	627685.93	9280425.48	45.00
2003	628635.66	9280619.75	47.00
2004	628863.10	9280200.42	49.20

Table 1: Coordinates of the extracted control points (Fluehler, 2004)

The control points were not distributed regularly over the two stereo models of the 1983 imagery, the southern part of the model area is completely uncovered. Especially the extraction of control points for planimetric orientation was a problematic process, presumably due to planimetric errors in the maps. Figure 3 shows the distribution of control points overlaid on the scanned 1:10.000 map, the extracted points are displayed in blue while the red points show the positions of control points for the orientation of the 1949 imagery. The rectangle contains the model area of the three 1983 images. Obviously no common control points could be used for the orientation of both series of aerial images. Due to the reasons mentioned above, the accuracy of point extraction from the 1:10.000 map is estimated to +/- 5m in the best case.

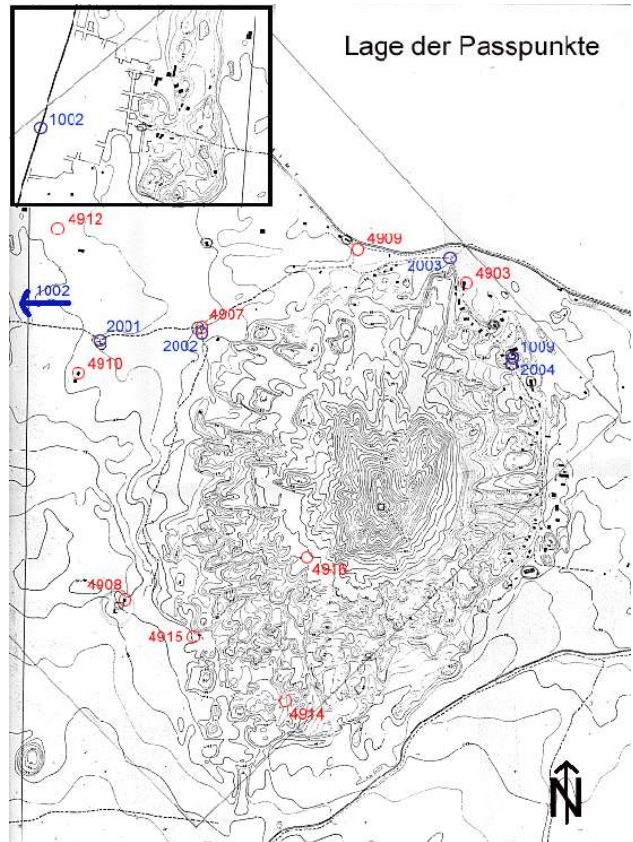


Figure 3: Control points for the 1983 images (blue) and the 1949 images (red), the rectangle shows the model boundaries of the images 598, 599 and 600 from 1983 (Fluehler, 2004).

2.2 Orientation of the 1983 images

The orientation of the 1983 images on an analytical plotter WILD S9 using AVIOSOFT's ATP aerotriangulation software requires the input of a camera file which contains the camera constant, coordinates of the fiducial marks, image format and lens distortion parameters taken from the calibration protocol. The camera used in 1983 was a Zeiss RMK 15. After the fiducial marks were measured and an affine transformation was applied to the measured coordinates of the fiducial marks, the inner orientation had been accomplished successfully with an accuracy of at least 6µm in all images. For relative orientation, tie points had to be measured in each stereo pair. To achieve a stable relative orientation, 15 tie points in von Gruber positions were measured in each model so that the y-parallaxes could be kept under 15µm. For absolute orientation, the extracted control points were measured in the images and the image coordinates of tie and control points together with the camera data and the object space coordinates of the control points were exported to BUN, IGP's internal bundle adjustment software. Performing bundle adjustment, a σ_0 of 18.51µm was achieved and the orientation parameters for the images re-imported to ATP.

2.3 Control point extraction from the oriented 1983 images

To obtain control points suited for an orientation of the 1949 images, corresponding points between both series of images had to be identified. In this step, 9 common points could be found

which could be used as full control points for orientation of the four 1949 images (Table 2). Anyway, it has to be taken into consideration, that the influence of the unfavourable distribution and the low accuracy of extraction of the first set of control points propagates fully to the second set.

ID	X [m]	Y [m]	Z [m]
4903	628690.96	9280528.76	45.52
4907	627647.36	9289368.74	44.38
4908	627284.81	9279373.86	49.10
4909	628127.41	9280773.00	43.72
4910	627169.09	9280203.06	44.96
4912	627119.46	9280739.93	41.18
4914	627838.67	9278921.06	53.63
4915	627536.07	9279254.34	47.55
4916	628085.84	9279428.11	65.09

Table 2: Coordinates of the control points for the 1949 images (Fluehler, 2004)

2.4 Orientation of the 1949 images on the analytical plotter

The 1949 images were oriented on both, the analytical plotter and the digital photogrammetric workstation Virtuozo 3.1. In this case, the definition of camera parameters had to be done based on assumptions because no information concerning the used camera was available. The characteristic shape of the fiducial marks in the images (Figure 4) belongs likely to a Fairchild camera, a common aerial camera in the 1940s (Smith, 1979).

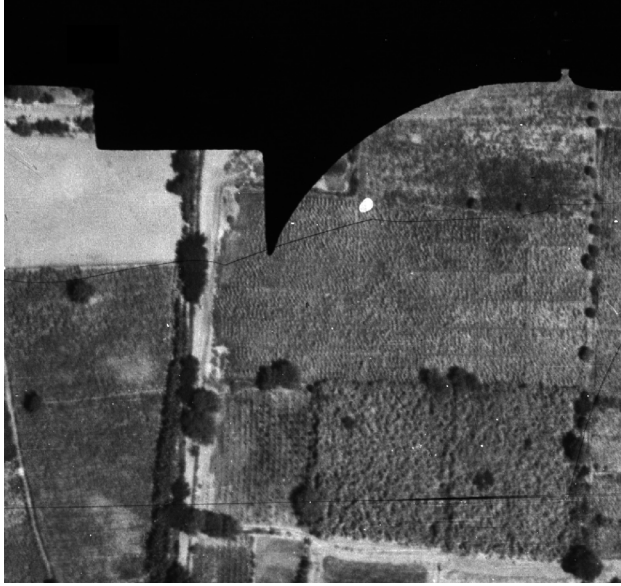


Figure 4: Fiducial mark as used in Fairchild cameras

Based on this assumption the camera constant was set to 152.4mm. Furthermore, the coordinates of the fiducial marks were measured in the image with millimetre-accuracy and taken as reference values for the inner orientation (Table 3). As a consequence, the accuracy of the affine transformation is worse by a factor 10 compared to an affine transformation on known, calibrated fiducial mark coordinates. The relative orientation was then accomplished analogous to the 1983 images while for the

absolute orientation only the single models were oriented using the control points and no bundle adjustment performed.

Fiducial	X [mm]	Y [mm]
1	0	-110.9
2	-108.8	0
3	0	110.9
4	108.8	0

Table 3: Approximative coordinates of the fiducial marks (Fluehler, 2004)

2.5 Orientation of the 1949 images using Virtuozo 3.1

The 1949 images, scanned at a resolution of $15\mu\text{m}$ in TIFF format using a Vexcel UltraScan 5000, first had to be imported into Virtuozo's internal VZ format. The camera parameters are given according to the analytical orientation mentioned in 2.4. As no matching template for the shape of the Fairchild fiducial marks exists in Virtuozo, the inner orientation has to be done manually. Again, the accuracy of the affine transformation is about a factor 10 worse than usual, using calibrated fiducial coordinates. For relative orientation, a 3x3 tie point pattern was chosen and an automated quality control applied to the automatically extracted tie points. The control points then were measured in semi-automated mode: after relative orientation it was sufficient to measure a point in one image, the corresponding point could then be matched automatically in the second image. After that, bundle adjustment was performed using PATB for the whole block with a global accuracy σ_0 of $3.07\mu\text{m}$ as a result.

3. DTM/DSM GENERATION

3.1 Manual DTM measurement on the analytical plotter

DTM measurement on the analytical plotter was performed using the AVIOSOFT XMAP software. The terrain points were measured in parallel profile mode, with a distance of 20m between the profiles. Along the profiles, considering the terrain, point density was increased if necessary, and, furthermore, breaklines were measured especially on the pyramids and *Cerro La Raya*. The masspoints and breaklines then were interpolated to a regular grid using DTMZ, a software developed at IGP based on bilinear finite elements interpolation, that performs Delauney-triangulation. A grid with a mesh size of 5m was interpolated.

3.2 Automated DSM generation with Virtuozo 3.1

Before DSM generation, based on the orientation results of the bundle adjustment, stereo models and epipolar images were created. First trials showed that additional breaklines and manually measured single points on the mountain ridge and slopes had to be integrated before matching to avoid gaps in the DSM. The problem occurred mainly on the mountain top, where the image is very bright (Figure 5) and lowly textured, therefore, no points could be matched correctly in this area without pre-knowledge.

After matching was performed, a quality control of the matched points could be accomplished using the "Match Edit" function of Virtuozo. The matched points are divided into three classes: green (reliably matched), yellow and red (unreliable). Figure 6

shows, that the unreliable points are mostly situated on slopes, especially the sidewalls of the pyramids and the mountain slopes are mostly red.



Figure 5: Mountain ridge of *Cerro La Raya*

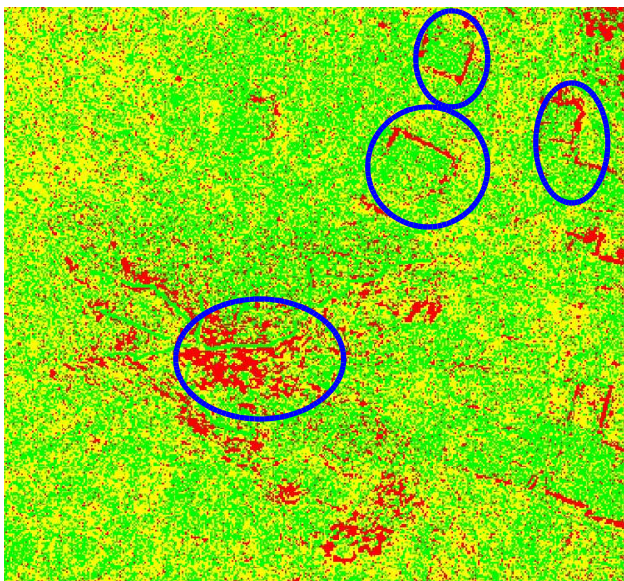


Figure 6: Reliability of matched points (green = reliable, red = unreliable), blue ellipses mark the critical areas

The derived contour lines and stereo viewing the critical points can be checked and edited if necessary. After matching achieved sufficient results, i.e. no blunders could be detected anymore, the DSM with a mesh size of 1m was generated for each stereo model. The three DSMs then were combined using the *Grid.Mosaic* command in ArcView 3.2.

3.3 Generation of the Orthomosaic

For the orthophoto generation, a footprint of 0.2m was chosen to provide a detailed view of the adobe architecture. The three geo-referenced orthoimages, each covering the whole model area accordingly, were exported to TIFF format with a worldfile containing the footprint and coordinates of the upper left corner of the image and then imported to ERDAS Imagine 8.6. With the mosaic tool, finally the three images were combined to one. The feathering function was applied to avoid visible boundaries inside the orthomosaic.

4. VISUALISATION

4.1 Skyline Terra Builder and Explorer Pro

From the derived DSM and orthomosaic, a photorealistic 3D model was produced using Skyline Terra Builder and Explorer Pro, version 3.0 (Sauerbier, 2003). The Terra Explorer Pro allows for a good real time navigation performance, especially in large terrain datasets. Figure 7 shows an overview of the central site of adobe architecture at Túcume as a still 3D view taken from the Terra Explorer Pro. Furthermore, the opportunity to produce pre-defined flight paths was used to generate different routes which then could be recorded to synthetic flyovers in AVI or MPEG format. For visualisation in Skyline, the DSM had to be resampled to a mesh size of 5m as the 1m grid could not be imported into the internal Skyline format MPT and to achieve a smooth surface.

4.2 ERDAS Imagine Virtual GIS 8.7

DSM and orthomosaic were imported to ERDAS IMG format in a second visualisation step. Compared to Skyline Terra Explorer Pro, ERDAS Virtual GIS provides less real time performance in terms of navigation speed in high resolution datasets, but offers the possibility to render very high resolution views from any observation point with high texture quality (Sauerbier, 2003). See Figure 8 for an example showing the largest adobe complex of the site, *Huaca Larga*.



Figure 7: 3D view of the Túcume adobe complex, produced with Skyline Terra Explorer Pro

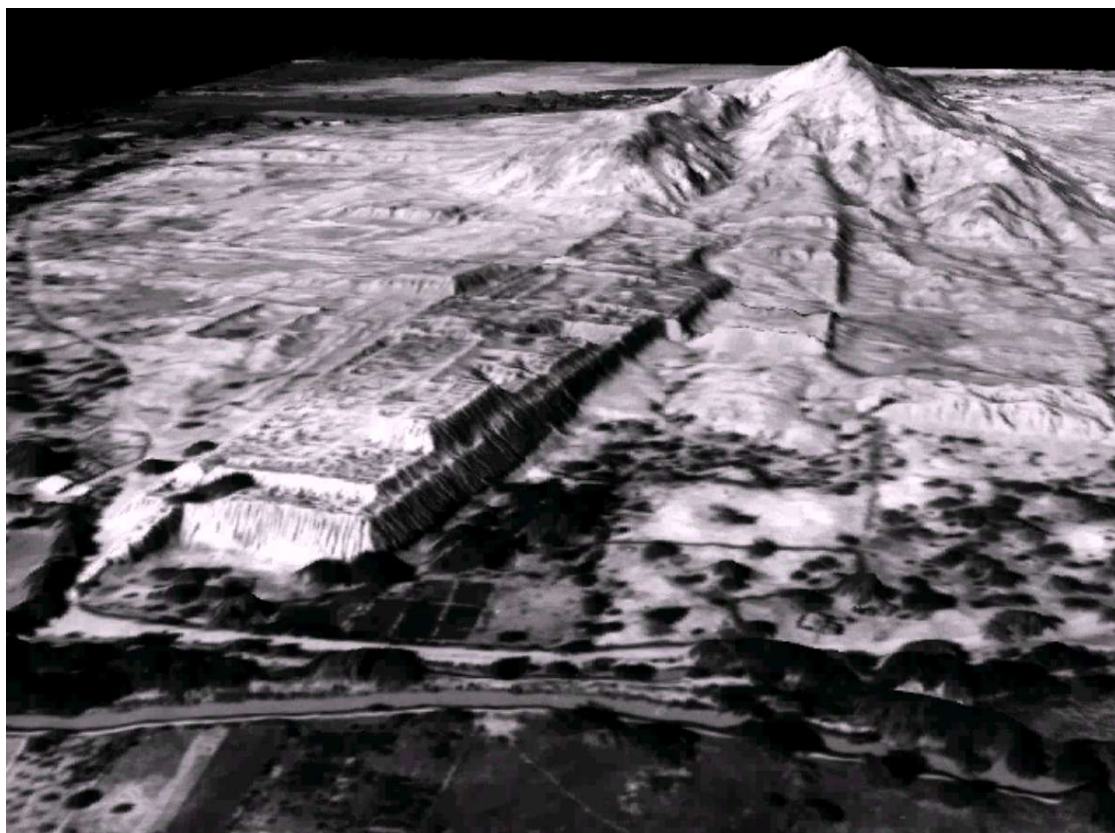


Figure 8: 3D view of *Huaca Larga*, produced with ERDAS Imagine Virtual GIS 8.7

4.3 Comparison of DTM and DSM

For a comparison of the manually measured DTM and the automatically generated DSM, both datasets were converted to ESRI grid format. Only the two southern stereo models were used for comparison. Afterwards, in ArcView 3.2 the difference grid

$$\Delta H = H_{DTM} - H_{DSM}$$

was calculated. As a result, a mean difference value of -0.68m with a standard deviation of 2.62m were obtained (Fluehler, 2004). Besides the fact, that the surrounding vegetation was

included only in the DSM, the main height differences between both datasets occurred in the area of *Cerro La Raya*. Here, not only a lack of texture influenced matching accuracy, but also image quality, as the images are too bright, especially near the mountain top. The errors mainly were situated at the mountain and pyramid slopes (Figure 9), as the ridges in both datasets were included as breaklines. Another effect, which can be identified in Figure 9, is a systematic shift between both datasets in approximately north-south direction. Furthermore, the northwest and the southeast corners of the compared area show large negative height differences, which may result from the poor distribution and small number of control points.

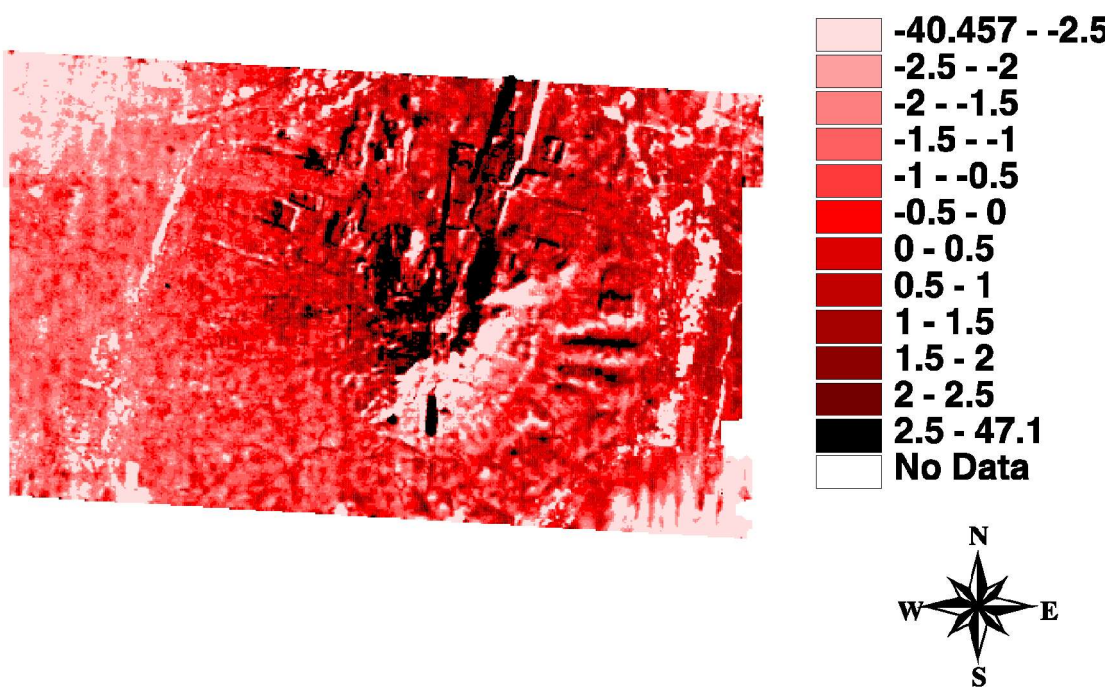


Figure 9: Comparison of DSM and DTM (Fluehler, 2004)

For a judgement of the absolute accuracy of both, DSM and DTM, no reference data of higher accuracy is available. Due to the unknown quality of the maps used for the extraction of control points, absolute accuracy remains an unresolved issue in this project.

5. CONCLUSIONS

This project provides a photorealistic 3D model of the pyramids of Túcume, in a state of preservation as of 1949, the earliest date aerial image data taken by metric cameras is available for. The model may serve as a means for documentation and presentation of the adobe complex in the local museum at Túcume or for scientists involved in the archaeological research. The preservation of the adobe complex as an important cultural and archaeological site in northern Peru, not only as a virtual model, is a goal Peruvian scientists are aiming for. The authors hope that the 3D model may be able to support their efforts.

6. ACKNOWLEDGEMENTS

The authors would like to thank Prof. Dr. Armin Gruen for his contributions to the project and Prof. Juan Reiser for initiating

this work. Furthermore, we thank Karsten Lambers for his archaeological advice.

7. REFERENCES

- Fluehler, M., Kunz, M., 2004. Generierung eines photorealistischen 3D-Modells von Túcume, Peru. Semester work, unpublished.
- Sauerbier, M., Lambers, K., 2003. A 3D model of the Nasca lines at Palpa, Peru. In: *International Archives of the Photogrammetry, Remote Sensing and Spatial Information Sciences*. Vol. XXXIV-5/W10.
- Smith, J., 1979. Manual of color aerial photography. ASPRS Virginia. Chief editor: John Smith.